ORIGINAL PAPER

# Metal ion-driven synthesis of polyaniline composite doped with metallic nanocrystals at the boundary of two immiscible liquids

**Marianna Gniadek · Elzbieta Bak · Zbigniew Stojek · Mikolaj Donten**

**Abstract** In this work, silver and gold–polyaniline composite materials were chemically synthesized at the nitrobenzene/water interface. Aniline (monomer) was dissolved in nitrobenzene and the oxidizing agent (either silver (I) or gold (III)) was dissolved in water. Metals, which were formed during the reaction were in nano- and microcrystalline forms and were partially embedded in the polymer. The forms of gold and silver crystallites found in the synthesized composites differed significantly. The rate of growth of the PANI-Ag and -Au composites and their morphologies depended on concentration of the reagents in both phases. The average size of the gold crystals was smaller compared to silver and was in the range of 20–25 nm. The obtained composite materials were characterized by cyclic voltammetry, scanning electron microscopy, and Raman spectroscopy. The pernigraniline species of polyaniline dominated in the entire volume of the PANI-Au composite and in parts of the PANI-Ag material located at the aqueous solution side, while partially oxidized emeraldine was the main component of PANI-Ag at the organic phase side.

**Keywords** Polyaniline composite · Silver · Gold · Liquid/liquid interface · Powder XRD · Scanning electron microscopy · Raman spectroscopy

M. Gniadek · E. Bak · Z. Stojek · M. Donten (✉)
Department of Chemistry, Warsaw University,
ul. Pasteura 1, 02093 Warsaw, Poland
e-mail: donten@chem.uw.edu.pl

Z. Stojek
e-mail: stojek@chem.uw.edu.pl

## Introduction

Among the known conducting polymers, polyaniline is unique due to its easy synthesis, relative environmental stability, and reversible acid–base chemistry in aqueous solutions. However, polyaniline is conductive only in the moderately oxidized state—emeraldine. To counter such a polymer problem, the incorporation of metal nanoparticles into the polymer may be done [1, 2]. By selecting the appropriate inorganic and organic phases for the synthesis of such composites, it is possible to design their specific properties [3, 4]. Several applications of inorganic–organic nanocomposites in conductometric gas sensors [5] and optical pH sensors [6], antirefractive coating, and organic batteries and micro electronics have been reported. Regarding polyaniline, Li and coworkers [7] obtained a new route for fabrication of platinum–polyaniline nanofilms at a liquid/liquid interface. This method enabled the incorporation of Pt nanoparticles into PANI by the simultaneous reduction of $H_2PtCl_6$ (emulsion in organic phase) to Pt nanoparticles and chemical oxidation–polymerization of aniline (water phase). The obtained PANI-Pt nanofilms exhibited an enhanced, potential-dependent conductivity. As for conductivity, PANI-Pt composite appeared to be a potential switchable material. Another approach to interfacial synthesis where platinum loaded polyaniline nanowires in poly(styrene sulfonic acid) were obtained was presented by Liu et al. [8]. In a different approach, Hirao and coworkers [9] used two methods of template synthesis to obtain a polyaniline/Pd nanoparticles material and employed it as a catalyst for the oxidative coupling reaction of 2,6-di-*t*-butylphenol.

A route for the synthesis of polyaniline/Ag nanocomposite was presented by Zhao and coworkers [10]. The core-

shell nanocomposites (Ag in PANI) were synthesized via the in situ chemical oxidation–polymerization of aniline based on the mercaptocarboxilic acid capped Ag-nanoparticle colloid. Another method to obtain the polyaniline/Ag nanoparticle material was that proposed by Song and coworkers [11] who used γ-ray irradiation for the oxidative polymerization of aniline-stabilized Ag colloids.

Other useful nanoparticles are the gold ones; they have good catalytic properties. Chattopadhyay and coworkers [12] reported a new method of solubilization of polyaniline–Au nanoparticles composite by encapsulating nanometer-size composites in starch. Yang and coworkers [13] synthesized water soluble polyaniline–Au nanocomposite by using 3-aminophenylboronic acid as a reductive and protonative reagent; polyvinyl alcohol (PVA) was used as disperser. The authors showed that the size of the particle can be changed by changing the concentration of PVA.

In the present work, polyaniline metal composites were chemically synthesized at liquid/liquid interfaces in one step process without using additional supporting chemicals. The monomer (aniline) was dissolved in nitrobenzene, and the oxidizing agents (appropriate silver or gold salts) were dissolved in the aqueous phase. Due to reasonable solubility of aniline in water, it is possible that a part of it can move to the water phase and react with metal ions next to the liquid/liquid interfaces. This procedure led to simultaneous occurrence of the polymerization of the monomer and of the reduction of metal ions at the liquid/liquid interface; the interfacial redox reaction was accompanied by the ion transfer through the phase boundary. So far, the liquid/liquid interfaces were mainly used to obtain just silver deposits of controlled morphology at the nitrobenzene/water and n-octanol/water interfaces by using silver nitrate in the aqueous phase, ferrocene, and decamethyloferrocene in the organic phase [14] and several other anions [15]. Although there are reports on the appearance of polyaniline at a liquid/liquid phase boundary [2, 16, 17], no works have been published on the preparation of PANI metal composites at a two-phase boundary. The composite materials which we obtained were characterized by scanning electron microscopy (SEM), X-ray energy dispersive spectroscopy, X-ray diffraction (XRD), Raman spectroscopy, and voltammetry.

## Materials and methods

Lithium perchlorate (LiClO$_4$) and silver nitrate (AgNO$_3$) were purchased from Fluka; nitrobenzene was purchased from Aldrich and other reagents (chloroauric acid, nitric acid, and perchloric acid) were purchased from POCh, Poland. All substances were of analytical grade purity. The aqueous electrolyte solutions were prepared using high purity water obtained from a Milli-Q Plus/Millipore purification system (conductivity of water, 0.056 mS cm$^{-1}$). All experiments were performed at 22 °C.

The optical observations during the polymerization process were carried out using a light microscope, Axio Observer (Zeiss, Germany).

The SEM images were taken with a LEO 435 VP microscope in Germany. The device was working at a low sample current to give the highest possible resolution. Under such conditions, the effect of charge up was diminished. The chamber pressure was 10$^{-6}$ Torr and to obtain the best quality images, the pictures were registered with 15 keV electron beam energy. Before exposing the samples to vacuum, they were washed with acetone and dried.

Cyclic voltammetry was done in the three-electrode system using an EG and G PARC, model 283 potentiostat. A platinum cylindrical electrode of 300 μm in diameter was served as the working electrode. A silver/silver chloride/ saturated KCl electrode ($E$=0.199 V versus SHE) was used as the reference electrode, and a platinum wire was used as the auxiliary electrode.

For the X-ray diffraction examination of the crystallites an X'Pert-MPD Bragg and Brentano diffractometer equipped with a copper X-ray tube (λ=1.54056 Å), a focusing incident beam monochromator, and a semiconductor strip detector was used.

For the analysis of the polymer in the polyaniline metal composites, a confocal microprobe Raman system (T46000, Jobin-Yvon-Spex, France) was used. The Raman microscope was equipped with a Kaiser holographic notch filter, a 1,800 grooves/mm holographic grating, and a 1,024×256 pixels liquid nitrogen cooled charge-coupled device (CCD) detector. The microscope attachment was based on an Olympus BX40 system with a 50× long-distance objective (LMPLFL50×/ 0.50). A Laser-Tech, model LJ800, mixed argon/krypton laser provided the excitation radiation of 647.1 nm.

## Results and discussion

For the polymerization reaction of aniline that occurred at the nitrobenzene/water interface, the monomer (aniline) was dissolved in the organic phase (0.5 M) while the aqueous phase contained either 1 M AgNO$_3$ or 0.05 M to 0.25 M HAuCl$_4$. The Ag$^+$ and AuCl$_4^-$ ions were employed as the oxidants. Since the polymerization of aniline requires acidic conditions, the aqueous phase was appropriately acidified. Hydrogen ions were introduced to the aqueous phase with Ag$^+$ ions in two ways; either the solution was acidified with 0.5 M HNO$_3$ before it was brought into contact with NB, or it was first placed over the NB phase and then acidified with a small amount of concentrated HNO$_3$. In both cases, the effect was similar; however, the second method of acidification led to somewhat faster polymerization. In the case of chloroauric acid, the solution contained also 1 M HCl.

Interface polymerization induced by Ag (I)

The initialization of the polymerization reaction could be easily seen after a few seconds as a turbidity of the organic liquid in the vicinity of the interface. Twenty-four hours after the start of the polymerization, a substantial amount of the polymer was already accumulated at the interface. The polymerization proceeded as long as the oxidant ions supporting the reaction were present (aniline was always in excess; $(Cv)_{AN} > (Cv)_{Ag+}$). After several days, when the reaction was slowed down, the color of the obtained deposit turned from dark green to brown, indicating some changes in the oxidation products. No reaction was seen between nitric acid and aniline solution and nitrobenzene.

The effect of aniline concentration in the organic phase on the growth rate of the polymer layer was investigated at the constant concentration of $Ag^+$ (1 M) in the aqueous phase. For this purpose, four aniline solutions in NB were prepared as follows—0.2, 0.3, 0.4, and 0.5 M. As it was expected, the fastest growth rate of the PANI-Ag layer was observed for the aniline concentration of 0.5 M and that monomer concentration was selected for the further studies.

The morphology of the obtained polymer layers was investigated by SEM. The structures of the layers depended on the polymerization time. After 1 h polymerization, the polymer structure was smooth and resembled an elastic film/membrane. As the polymerization reaction advanced the polymeric layer became thicker (circa 100–300 µm after several hours of polymerization) and more porous but never reached the state of powder. The environment of the polymeric layer had an influence also. The structure of the polymer facing NB was smooth and rather compact while that facing the aqueous phase was fibrous and porous (see image B in Fig. 1).

Silver was partially incorporated into the structure of growing polymer net in the form of clusters and nanocrystals. A part of silver deposit formed separate phases—lamellas and whiskers of thickness in the range of 10 to 100 nm. Some of those structures were a fraction of millimeter long. Figure 2a, b presents two SEM images of different forms of obtained metallic silver after a 7-day synthesis. Long ribbons and small plates decorated with very small spheres at the edges are seen well in the figure. These were the dominated forms of metallic silver inclusions. A comparison of photos in Figs. 1 and 2 indicates the strong influence of polymerization time on the structure of the composite.

Next, the electrochemical characteristic of the obtained polymer layers was examined. The polymer generated at the water/NB interface was collected and placed onto a platinum electrode of 300 µm in diameter. To improve the pickup of the material from the interface, this platinum electrode was loop-shaped, and the plane of the loop was oriented parallel to the liquid/liquid interface. Only a thin polymer layer obtained after a short polymerization time could be transferred directly
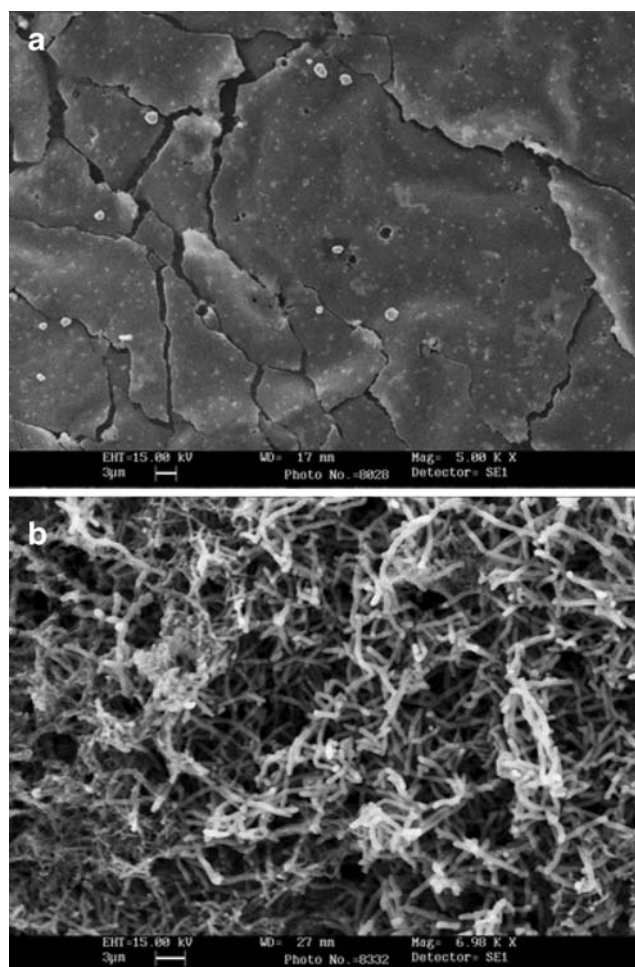


**Fig. 1** SEM images of polymer structures present at **a** nitrobenzene side and at **b** aqueous phase side of liquid/liquid interface. Concentrations—1 M $Ag^+$ and 1 M $HNO_3$ in aqueous solution; and 0.5 M aniline in nitrobenzene. Polymerization time—1 h

onto the electrode surface. Subsequently after the transfer, the electrode with the polymer was washed by dipping in acetone and water (was not dried) and immersed into 0.1 M aqueous solution of $LiClO_4$ acidified with $HClO_4$. Thicker layers could be only wrapped into a soft graphite rod. Figure 3 presents a typical cyclic voltammograms of PANI obtained at the phase boundary (curve a in Fig. 3). Curve a (Fig. 3) exhibits three pairs of peaks at 0.2 V, 0.45 V, and 0.7 V, respectively. In order to identify these peaks, cyclic voltammograms of pure PANI (obtained by voltammetric sweeping in the acidified monomer solution, curve b in Fig. 3) and $Ag/Ag^+$ couple (curve c in Fig. 3) were recorded separately and added to the figure. A comparison revealed that the first pair of peaks of the composite corresponded to the oxidation/reduction of the leukoemeraldine/emeraldine system, the second pair—to the oxidation/reduction of the silver couple, and the third pair—to the oxidation of the emeraldine/pernigraniline system. Regarding the middle Ag/Ag+ couple in the voltammogram; under the scan rate
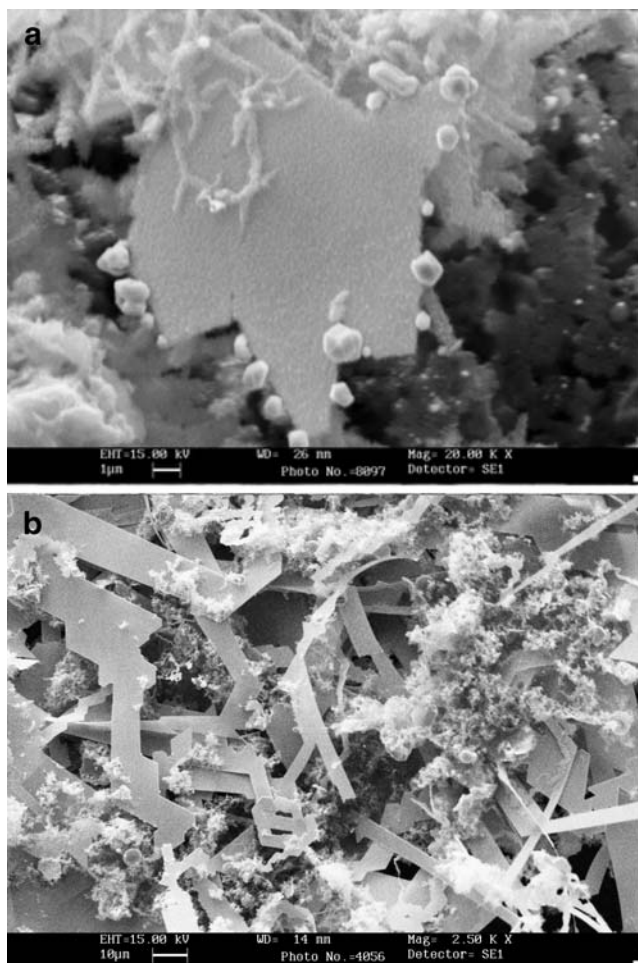
Fig. 2 Two SEM images of different magnification of various forms of metallic silver. Concentrations—1 M Ag$^+$ and 1 M HNO$_3$ in aqueous solution; and 0.5 M aniline in nitrobenzene. **a**, **b** represent two selected locations in the composite. Polymerization time—1 week

employed it is rather, impossible for silver ions to move completely out of the electrode surface, and the presence of the polymer may help keep the silver ions, so the reduction peak of Ag$^+$ appears in the voltammogram. The height of silver peaks is circa two orders of magnitude bigger compared to what might be expected for the formation of the Pt oxide layer; the total area of the Pt wire in the loop is circa 0.02 cm$^2$. The shape of the possible anodic peak of polycrystalline Pt will never be so thin as that of oxidation of nanoparticles of silver. The difference in the hydrogen evolution reaction, seen as the earlier rise of the reduction current, can be attributed to imperfect coverage of the polymer layer of the platinum surface.

Interface polymerization caused by Au (III)

The standard potential of the AuCl$_4^-$/Au couple is higher than that of Ag/Ag$^+$, thus, the polymerization reaction runs faster and its product appears in shorter time. Optimal concen-

trations of the gold salt for the synthesis were found to be from 0.05 to 0.25 M, and constant concentration of the hydrochloric acid was used (1 M). The obtained deposit differed from PANI-Ag. Metallic gold was spread more uniformly compared to PANI-Ag, and ribbons and foils were never seen. Typical morphology of the composite layer on the aqueous solution side is seen in Fig. 4a. This morphology is defined by the porous structure of the composite and granules of Au. In Fig. 4b, only small nanocrystals of Au (up to 20 nm) are seen. A selected granule consisting of many small nanocrystals is presented in Fig. 4c. In longer polymerization times, the number of granules increases. It can be due to lowering of the rate of composite formation, which enables the formation of larger metal structures. In the early stages, when the formation of the composite was fast, metallic gold was better dispersed in the polymer net, and fewer granules were seen. Only one property of two composites was similar: the nitrobenzene side of both composites surface was smoother than the water side.

Since it was not easy to load a thin layer of PANI-Au on the electrode surface, as it was done for PANI-Ag, the samples of polyaniline–Au taken for the electrochemical examination were washed with acetone, ethanol, and water and finally dried. Each sample was then rubbed into the surface of a graphite electrode. The rubbed-in material was examined using cyclic voltammetry. The results of the experiments are shown in Fig. 5. For the investigated material, the broad reduction and oxidation signals typical for polyaniline were obtained. For the comparison purpose, a cyclic voltammogram reflecting the behavior of the voltammetrically synthesized PANI is added to Fig. 5.
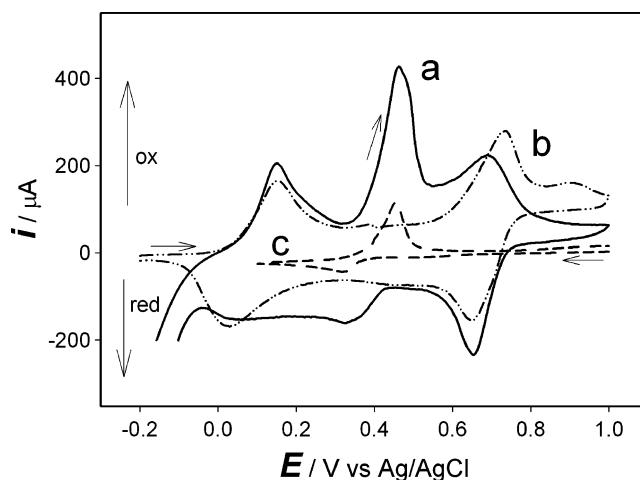


Fig. 3 Cyclic voltammograms of **a** PANI-Ag obtained in chemical reaction; **b** PANI obtained by cyclic voltammetry in 0.5 M aniline with 0.1 M LiClO$_4$ and 0.5 M HClO$_4$; and **c** oxidation and reduction of silver. Working electrode (a loop of 3 mm in radius made of 300 μm Pt wire, area of circa 0.18 cm$^2$) with sample of PANI immersed in—0.1 M LiClO$_4$ and 0.5 M HClO$_4$ (**a**, **b**). Bare Pt electrode in 1 mM AgNO$_3$, 0.1 M LiClO$_4$, and 0.5 M HClO$_4$ (**c**). Scan rate—50 mV/s
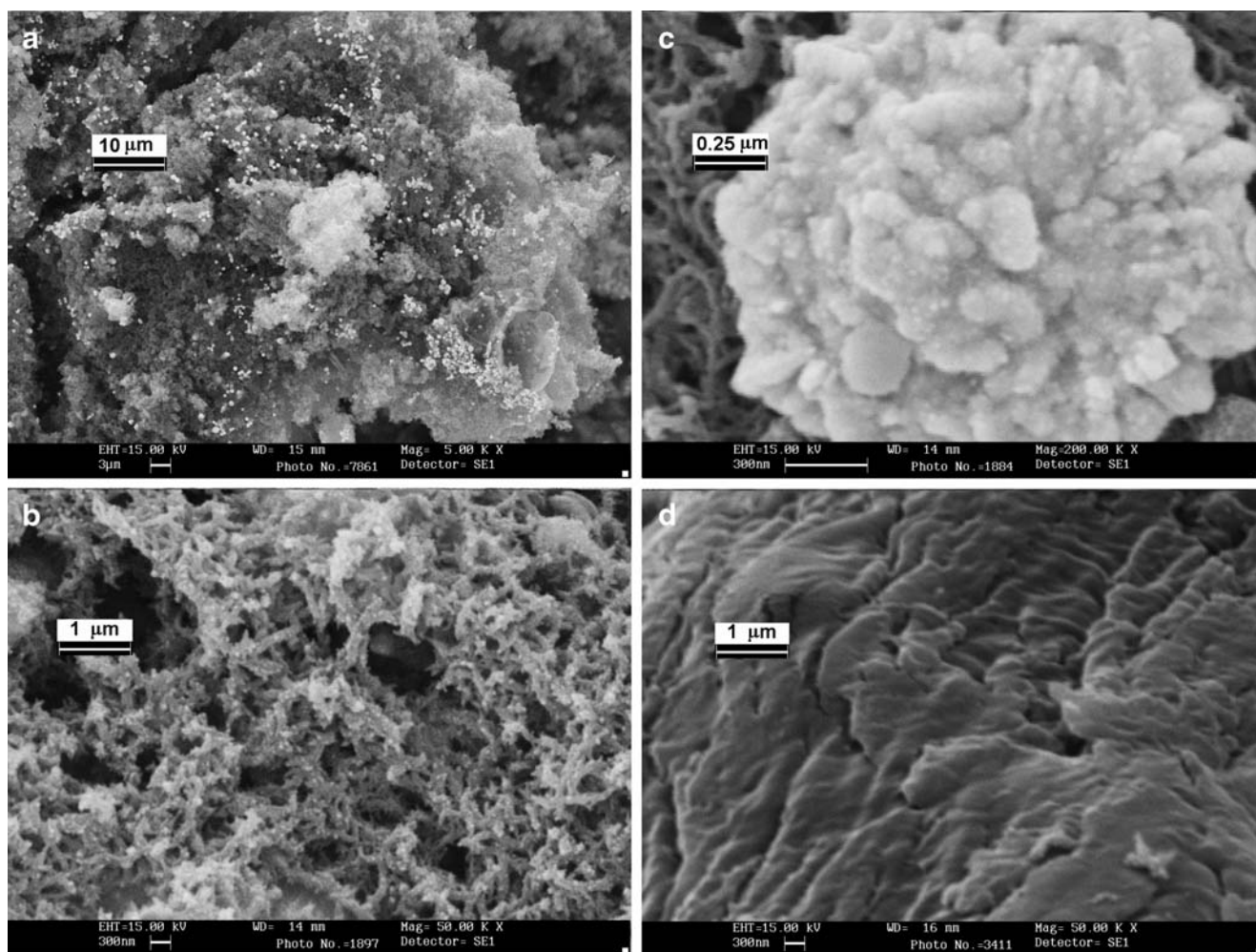
**Fig. 4** SEM images of different magnification of PANI-Au composite. Polymerization time—1 h; concentrations—0.25 M AuCl$_4^-$, and 1 M HCl in aqueous solution; 0.5 M aniline in nitrobenzene. Composite layer seen from the aqueous solution side (**a**, **b**) and magnified gold granule (**c**). Morphology of the layer in contact with nitrobenzene (**d**)
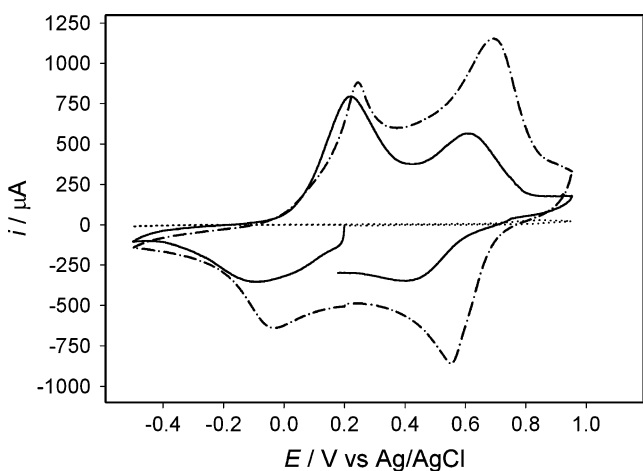


**Fig. 5** Cyclic voltammograms of gold-doped polyaniline rubbed into graphite electrode (*solid line*). Electrochemically deposited PANI (*dashed–dotted line*). Scan rate—0.5 V/s; 1 M LiClO$_4$. *Dotted line*– background

## Raman spectroscopy of composites

The polymer that was generated at the NB/water interface was green, and therefore, it was recognized as partially oxidized emeraldine. However, the existence of the fully oxidized pernigraniline in the composite could not be excluded. To find out which PANI species were formed during chemical polymerization of aniline doped with silver ions, the Raman spectroscopy was applied. For this purpose, the PANI-Ag composite samples were placed onto a ceramic clean and dry disk. Examined polymer was previously washed several times with water and left to dry for circa 1 h at 22 °C. All Raman spectra were recorded at the same wavelength 647 nm (red line). First, the spectra of the clean ceramic support were registered. Among the spectra of the composite, two different types can be distinguished; they are shown in Figs. 6a and 7a (water and nitrobenzene side, respectively). These spectra are identical to those published in the literature for the polymer
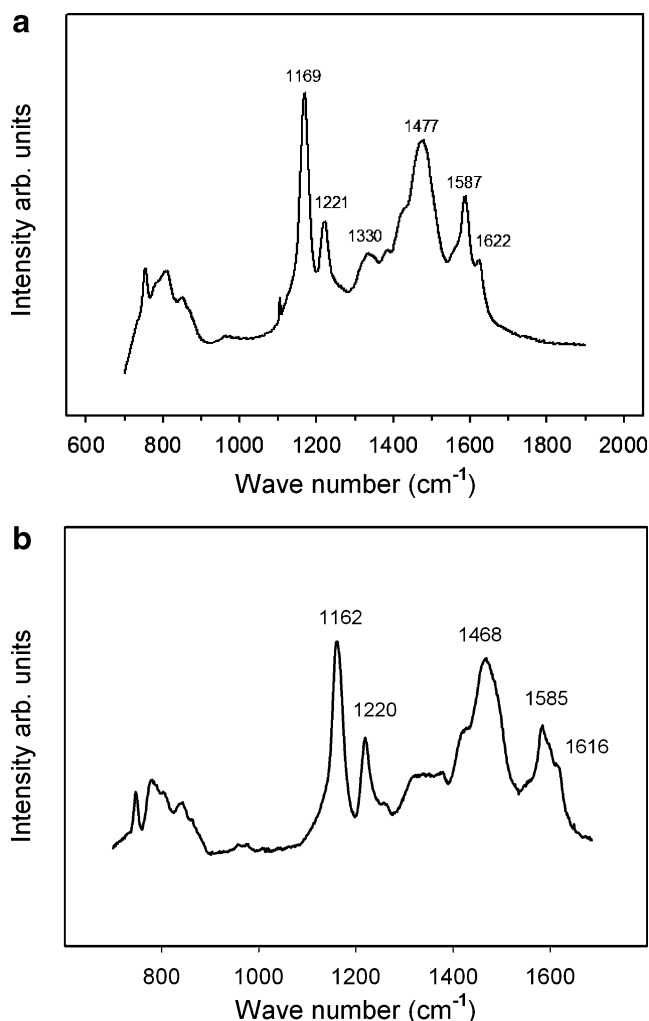
**a**

**b**

**Fig. 6** Raman spectra of a layer of PANI-Ag and electrochemically obtained PANI. *Exciting line*—647.1 nm. Spectra taken for **a** PANI-Ag composite located at water side (pernigraniline) and **b** electrochemically obtained pernigraniline

pernigraniline and to higher (1,173) for emeraldine. Also, a comparison of other sections of the Raman spectra indicates that in the spectra in Fig. 7a, the intensity of characteristic bands of emeraldine is much stronger than that of the signals of pernigraniline. The increase of the band intensity at 1,325 cm⁻¹ from the emeraldine cation radical and the simultaneous deterioration of the band close to 1,490 cm⁻¹ for the C = N bond in the chinoid ring of pernigraniline confirm the higher content of emeraldine in the composite at the NB side. The above discussion is based on the literature data [18–21]. The above observation confirms the coexistence of emeraldine and pernigraniline in the polymer deposit formed at the NB/water interface. Importantly, since the silver ion cannot enter the nitrobenzene phase, while aniline can penetrate the aqueous phase, the polymer growth advanced towards the aqueous phase, which was rich in the Ag⁺ ions needed for the oxidation. Consequently, at the aqueous solution side, the completely oxidized form of PANI
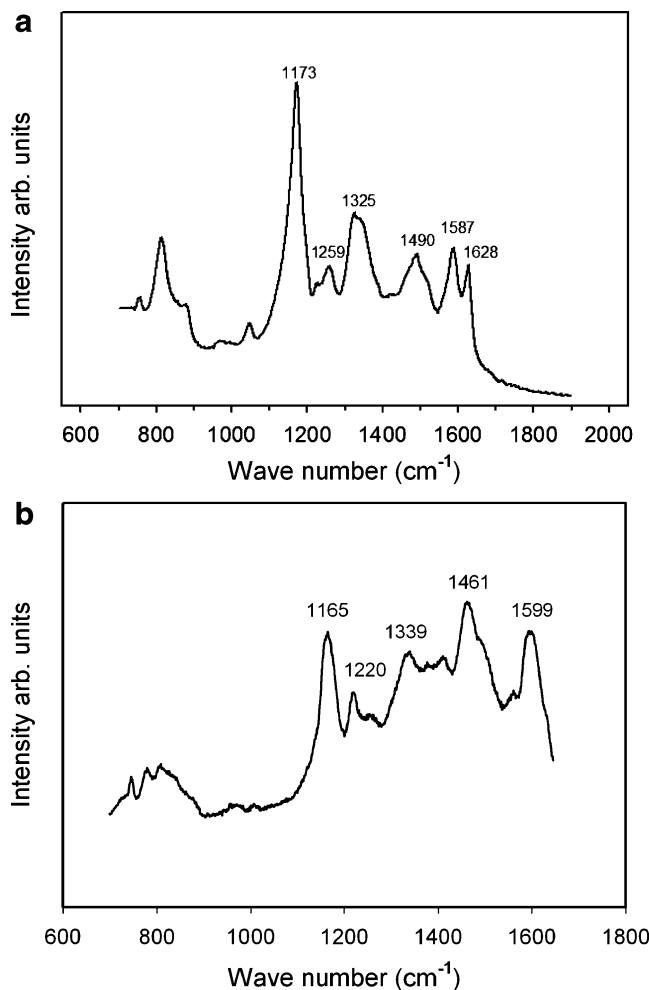


**a**

**b**

**Fig. 7** Raman spectra of a layer of PANI-Ag and electrochemically obtained PANI. *Exciting line*—647.1 nm. Spectra taken for **a** PANI-Ag composite located at organic liquid side (emeraldine) and **b** electrochemically obtained emeraldine

species (emeraldine and pernigraniline) obtained by electrochemical deposition. The signal of the support was very weak and is not visible in the spectra. In the spectra shown in Fig. 6a, the peaks corresponding to the fully oxidized pernigraniline dominate. The occurrence of this form of the polymer is confirmed by the presence of intense bands at 1,477 cm⁻¹ and 1,587 cm⁻¹, corresponding to the C = N stretching vibrations of bipolaron and C = C stretching vibrations in the chinoid ring, respectively. Also the band at 1,221 cm⁻¹ reflecting the C-N stretching vibrations are quite intense. The intensity of these vibrations weakens if the transition form of the polymer predominates in the investigated region of the deposit. The band at 1,330 cm⁻¹ is a characteristic for the radical cation of emeraldine. The band close to 1,170 cm⁻¹ represents the C-H bending vibrations in the aromatic ring and is present in the spectra of both polyaniline forms. This band, due to the changes in oxidation state of the polymer, shifts to slightly lower values (1,169) for

(pernigraniline) dominated, while the polymer deposited at the organic phase side consisted mainly from the less oxidized form—emeraldine. For the purpose of comparison, typical spectra of electrodeposited two forms of PANI have been added to Figs. 6 and 7.

Similar spectroscopic experiments done with the polymer obtained in the reaction with $(AuCl_4^-)$ proved that for synthesized polyaniline, in all locations, pernigraniline is the dominant form of the polymer. At some places, the samples look like metallic gold; however, the Raman spectra taken at these places are intensive and indicate the presence of the polymer. It is possible that in some places the noncovered gold could be present in the composite; however, the Raman spectra taken from the surface of the gold granules always indicated the presence of the polymer.

### Comparison of size and shape of Ag and Au crystals

Bulk gold and silver have the same crystallographic structure and similar lattice parameters; so, their powder XRD spectra should look similarly. However, the diffractograms obtained for the composite materials of Au and Ag differ. Typical X-ray diffractograms obtained for the composite samples containing Au and Ag are presented in Fig. 8. For both materials, the peaks are somewhat broader, and the ratio of intensity of silver signals is significantly disturbed. The signal related to Ag(111) should be the most intensive one and should be approximately three times more intensive than the signal of Ag(200). The very strong signals related to planes 200 and 400 suggest that the 100 orientation of the silver crystals (which is not active in XRD) is preferred in the analyzed sample. This can be caused by the nonuniform growth of the Ag crystals during the reduction of the $Ag^+$ ions by aniline. In fact, most of the silver deposits obtained during the formation of PANI-Ag composite appeared in a form of ultra



**Fig. 8** Powder XRD diffractograms of PANI-Ag and PANI-Au

thin ribbons or plates. The thickness of such objects, estimated from the SEM images, is circa 20–30 nm. It is probable that they have a structure of monocrystals with preferred one plane. This kind of abnormalities in the powder XRD patterns disappeared when the PANI-Ag samples were fragmented before measurements.

The ratio of intensities of the signals seen at the diffractograms taken with the PANI-Au composites does not indicate the existence of the disturbances observed in the Ag patterns. The broadening of the Au and Ag peaks can be explained by a significant drop in the size of the gold crystals incorporated into the composite. The equation proposed by Scherrer many years ago [22] that combines the half width of the diffraction peak with the size of the crystals present in the investigated substance is apparently useful in current investigations of crystalline objects [23, 24]. An analysis of the broadening of the Au(111) peak and the Au(200) peak indicated that the size of the gold crystals is in the range of 20–25 nm. The results of these calculations are consistent with the SEM data. Also, an estimation of the crystal size done by Bruker's commercial software TOPAS 3 indicated that gold incorporated into PANI-Au composite appears as circa 20 nm nanocrystals symmetrically spread in all directions. A full analysis of broadening of all diffraction peaks that appeared in the XRD spectra of Ag in the PANI-Ag composite indicated some differences in the crystal dimensions along various crystallographic planes. The biggest value (over 80 nm) was obtained for plane 100 (broadening of peaks, 200 and 400). The dimensions of silver crystals along other directions were smaller (20 to 30 nm). Those results met the SEM observations, which indicated the existence of ultra thin ribbons and flakes of silver in the PANI-Ag composite formed at the liquid/liquid interface (see Fig. 2).
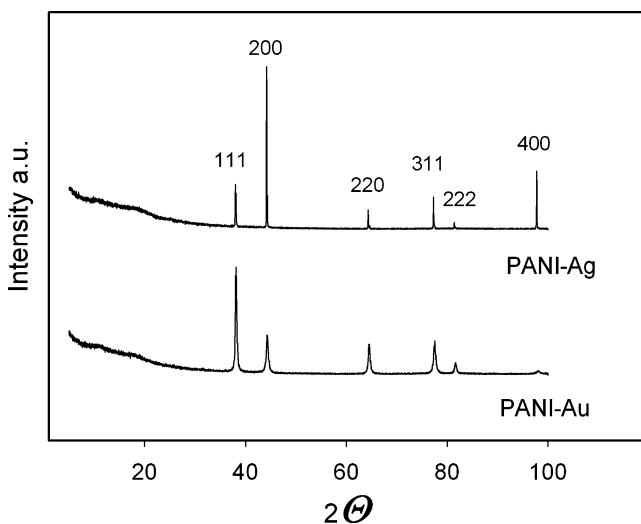
### Conclusions

In this work we have presented a simple, one step synthesis of conductive polymer-metal composites without using supporting chemicals. Depending on the metal ion used for the synthesis of the composite and on the conditions of the process, a variety of micro and nanostuctures of metals were obtained. The composites containing gold were more uniform, and the metal incorporated into polyaniline appeared to be practically in one structure granules made of nanocrystals of circa 20–30 nm in diameter.

The predominant forms of silver in the PANI-Ag composites were ultra thin ribbons and foils. The thickness of those objects estimated from the SEM images was in the range of 30–40 nm. The powder XRD data indicated that those flat objects had strong 100 texture.

Polyaniline present in the PANI-Ag and Au composites appeared mainly in the oxidized form—pernigraniline; how-

ever, in the composites formed with silver, some amount of emeraldine was also found in the deposit obtained at organic liquid side. The electrochemical properties of PANI metal composites synthesized at the liquid/liquid interface were examined after transferring them to the surface of either platinum or graphite electrodes. The polymers indicated the electrochemical activity typical for polyaniline.

## References

1. Sarma TK, Chowdhury D, Paul A, Chottopadhyay A (2002) Chem Commun 10:1048
2. Neoh KG, Young TT, Looi NT, Kang ET, Tan KL (1997) Chem Mater 9:2906
3. He Y, Lu J (2007) React Funct Polym 67:476
4. Athawale AA, Bhagwat SV, Katre PP, Chandwadkar AJ, Karandikar P (2003) Mater Lett 57:3889
5. Sadek AZ, Włodarski W, Kalantar-Zadeh K, Baker C, Kaner RB (2007) Sens Actuators A 139:53
6. Jin Z, Su Y, Duan Y (2000) Sens Actuators B 71:118
7. Zheng L, Li J (2005) J Electroanal Chem 577:137
8. Liu FJ, Huang LM, Wen TC, Gopalan A, Hung JS (2007) Mater Lett 61:4400
9. Amaya T, Saio D, Hirao T (2007) Tetrahedron Lett 48:2729
10. Jing S, Xing S, Yu L, Wu Y, Zhao Ch (2007) Mater Lett 61:2794
11. Kang Y-O, Choi S-H, Gopalan A, Lee K-P, Kang H-D, Song YS (2006) J Non-Cryst Solids 352:463
12. Sarma TK, Chattapadhyay A (2004) Langmuir 20:4733
13. Ma Y, Li N, Yang Ch, Yang X (2005) Colloids and surfaces A: physicochem. Eng Aspects 269:1
14. Scholz F, Hasse U (2005) Electrochem Commun 7:541
15. Scholz F, Gulaboski R (2005) Chem Phys Chem 6:16
16. Huang J, Virij S, Weiller B, Kaner R (2003) J Am Chem Soc 125:314
17. He Y (2005) Mater Sci Eng B 122:76
18. Baibarac M, Cochet M, Łapkowski M, Mihut L, Lefrant S, Baltog I (1998) Synth Met 96:63
19. Baibarac M, Mihut L, Louarn G, Lefrant S, Baltog I (2000) J Poly Sci B 38:2599
20. Berrada K, Quillard S, Louarn G, Lefrant S (1995) Synth Met 69:201
21. Arsov LjD, Plieth W, Koßmehl G (1998) J Solid State Electrochem 2:355
22. Patterson AL (1939) Phys Rev 56:978
23. Alexandrov IV, Enikeev NA (2000) Mater Sci Eng A 286:110
24. Donten M, Stojek Z, Cesiulis H (2003) J Electrochem Soc 150(2): C95